# Corrosion and protection of thin-line conductors in VLSI structures

by V. Brusic

G. S. Frankel

C.-K. Hu

M. M. Plechaty

G. C. Schwartz

Thin metallic lines in VLSI circuit structures are usually encapsulated in a dielectric in order to protect them from the atmosphere and prevent corrosion. However, during processing the lines are unprotected. Some of the steps to which they are subjected during processing are quite aggressive and can result in a significant yield loss. This paper pertains to the loss which is due to corrosion during processing. It focuses on the corrosion behavior of the two of the most commonly used conductors, aluminum and copper. Aluminum alloyed with small amounts of copper is also considered. The corrosionrelated behaviors of aluminum and copper are vastly different, as is shown by their reaction with water and several processing solutions. The challenge of minimizing corrosion during processing as well as during subsequent storage and use is discussed, using suitable examples drawn from studies of thin films of

the metals exposed to chemical etching, reactive ion etching, and cleaning.

#### Introduction

The purpose of this paper is twofold. First, a brief summary of the fundamental aspects of electrochemistry of corrosion is presented. The interested reader may find more details in the literature [1–6]. Second, some of the specific concerns in fabricating interconnections for very large scale integrated (VLSI) circuits are discussed. VLSI circuit fabrication often calls for the use of harsh chemicals, and it is important that both processing and postprocessing steps do not cause unwanted and uncontrolled corrosion. The interconnections of such circuits are most commonly fabricated with Al-Cu alloys [7], while Cu metallization is being considered for future use [8, 9]. After a brief discussion of the experimental approaches used, examples are given of relevant studies of 1) the corrosion and protection of Al-Cu and Cu in neutral and nearly neutral electrolytes, 2) the effects of HF, 3) the

<sup>e</sup>Copyright 1993 by International Business Machines Corporation. Copying in printed form for private use is permitted without payment of royalty provided that (1) each reproduction is done without alteration and (2) the Journal reference and IBM copyright notice are included on the first page. The title and abstract, but no other portions, of this paper may be copied or distributed royalty free without further permission by computer-based and other information-service systems. Permission to republish any other portion of this paper must be obtained from the Editor.

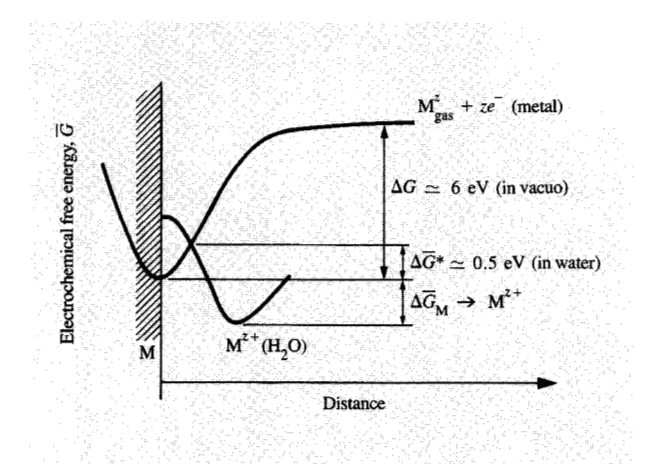


Figure 1

Driving force for corrosion.

corrosion of Al-Cu and Cu films after reactive ion etching (RIE), and 4) the etching and protection of Cu films.

# Fundamental aspects of corrosion reactions

# • Thermodynamics and kinetics

Corrosion may be described as the loss of metallic mass and properties as a result of spontaneous reactions with the environment. The formation of a corrosion product is a consequence of metallic oxidation, which occurs with the simultaneous reduction of other available reactants, notably hydrogen ions or dissolved oxygen [1, 2]. The overall process is similar to the processes that occur in a short-circuited battery: It is an electrochemical process that wastes both material and energy. The corrosion of aluminum in water can be expressed as

$$Al + 3H_2O \rightarrow Al(OH)_3 + 3/2H_2$$
 (1)

or

$$AI \rightarrow AI^{+3} + 3e^{-}, \tag{2a}$$

$$3H^+ + 3e^- \rightarrow 3/2H_2$$
, (2b)

with oxidation [Equation (2a), corrosion, anodic reaction] typically occurring nanometers away from the reduction [Equation (2b), cathodic reaction]. The second reaction, reduction, is rarely observed visually. However, in its absence corrosion would not occur.

Corrosion is very dependent on the environment, i.e., the source and nature of the cathodic reactants that are present. In the absence of oxygen and water, the energy required to form metal ions (gas) and electrons is of the order of 6 eV [2] (see Figure 1). Therefore, in vacuum,

metals are stable with regard to corrosion. Additionally, corrosion does not occur under conditions under which the arrival of these reactants to the metallic surface is prohibited (e.g., under perfectly protective overcoats). However, in a normal process ambient, in which water and oxygen can reach the metallic surface, corrosion does occur at some finite rate. In aqueous environments metal ions are solvated by water molecules. Because this is an energetically favorable state, the corrosion of most metals in aqueous environments is not only a spontaneous process, but one which has a relatively low energy of activation (about 0.5 eV), as indicated in the figure.

The corrosion process involves a transfer of charge a redistribution of ions and electrons—requiring an expenditure of work. The total energy possessed by a charged entity is

$$\bar{G} = G + (ze^{-})\Phi, \tag{3}$$

where  $\overline{G}$  is its electrochemical free energy, G is its chemical free energy,  $ze^-$  is its charge [with z being the change of ionic charge in an electrode process, as described by Equations (2)], and  $\Phi$  is the electrical potential in the point in space where the entity is located. It follows that the work required to move an electric charge of  $ze^-$  units from one point to another, where the electrical potential differs by  $\Delta\Phi$ , is  $(ze^-)\Delta\Phi$ . At equilibrium, the energy content of reactants and products is the same and  $\Delta \overline{G}=0$ . Hence, the net change in chemical free energy is an exact balance of the electrical work required for the ion to traverse the electrode/electrolyte interface, and

$${}^{0}\Delta^{+}\Phi = {}^{+}\Delta^{0}G/ze, \tag{4}$$

where  ${}^{0}\Delta^{+}$  and  ${}^{+}\Delta^{0}$  denote the change (of either potential or chemical energy) from the metallic to oxidized state or vice versa. This equilibrium potential difference is a characteristic of the specific metal electrode. The oxidation-reduction potentials (also known as half-cell potentials) and the electromotive force or EMF series can be measured on a relative scale and can be used to predict whether or not a metal will corrode in a given environment [1]. This is accomplished by the following generalized rule: In any electrochemical reaction, the most negative half-cell tends to be oxidized and the most positive half-cell tends to be reduced. Some of the standard oxidation-reduction potentials are listed in Table 1 [1, 4, 5], with respect to a normal hydrogen electrode (NHE). Table 1 indicates that Al should corrode in acidic media, while copper should be a good container material for de-aerated acids, a prediction which has been observed to be correct. In the presence of oxygen and the absence of complexing ions, only gold is expected to be totally unreactive, or "noble." Although thermodynamic arguments can be used to predict whether or not corrosion should occur, to estimate the composition

174

of the corrosion products, and to predict environmental changes which should prevent or reduce the corrosion attack, the kinetics of all the participating reactions, and not just thermodynamic aspects, determine the overall extent of corrosion.

The reaction rate is proportional to the probability that the reactive species are able to surmount the energy barrier. In an electrochemical process, the rate of a chemical change is proportional to a flow of charge; hence, the reaction rate can be measured as a current per unit area, i.e., current density *i*. This is a more effective way to follow the reaction rate than using alternative methods (e.g., by determining a mass change). Furthermore, the activation energy depends on electrode potential, as indicated by Equation (3). Consequently, the general expression for the reaction rate of an electrochemical process can be expressed as

$$i = i_0 \exp(zF\alpha\Delta\Phi/RT), \tag{5}$$

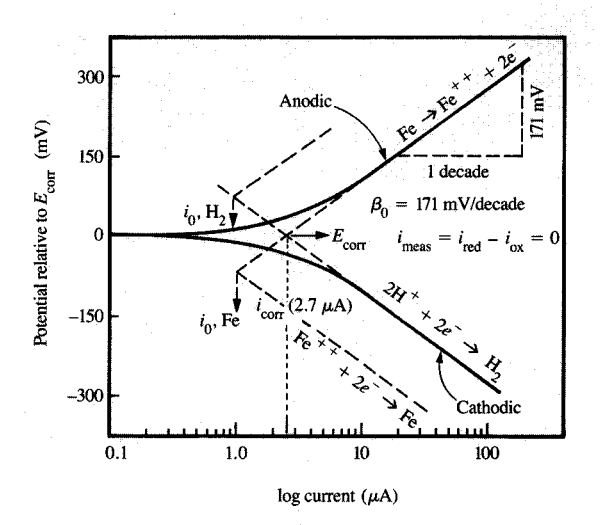
where  $i_0$  is the exchange current density or reaction rate at the equilibrium potential, z is the ionic charge,  $\alpha$  is the symmetry coefficient which describes the shape of the rate-controlling energy barrier, F is the Faraday constant,  $\Delta\Phi$  is the overpotential, or the potential difference between the applied and equilibrium potentials, R is the gas constant, and T is the temperature at which the process occurs.

Metal is dissolved as the potential increases above the equilibrium potential, or, in reverse, metal ions can be plated at the cathodic potentials. At potentials some 50 mV or more removed from the equilibrium potential, a linear relationship is observed between the logarithm of the current and the potential (Tafel region), as predicted by Equation (5), namely

$$\Delta \Phi = b \log i / i_0 \,, \tag{6}$$

where b is the Tafel slope. This aspect of the reaction kinetics, in which the reaction rate varies with the potential, is the single most important difference between chemical and electrochemical kinetics. The rate of electrochemical reactions can be drastically affected by a relatively small change of the potential. For instance, with a Tafel slope of 60 mV/decade and a symmetry factor of 0.5, an increase in potential of 0.5 V causes an increase of the reaction rate by eight orders of magnitude!

The corrosion rate is a consequence of at least two spontaneous reactions: metal dissolution following anodic kinetics, and the reduction of an available oxidizing agent following the cathodic kinetics characteristic for the given metallic surface. Figure 2 shows reactions relevant to the corrosion of iron in acidic solutions. The exchange current density for hydrogen evolution on iron is about  $1 \times 10^{-6}$  A/cm<sup>2</sup>, similar to the exchange current density for iron dissolution and deposition. Placed in a de-aerated acidic solution, iron will dissolve as fast as hydrogen can evolve.



#### Floure 2

Electrochemical kinetics of metallic dissolution, hydrogen evolution, and the corrosion potential and rate; relevant to the corrosion of iron in acidic solutions.

**Table 1** Standard electrochemical potentials [1, 4, 5].

Metallic state	Potential (V vs. NHE)
$K \rightarrow K^+ + e^-$	-2.92 (active)
$Na \rightarrow Na^+ + e^-$	-2.71
$Mg \rightarrow Mg^{+2} + 2e^{-}$	-2.38
$Al \rightarrow Al^{+3} + 3e^{-}$	-1.66
$Zn \rightarrow Zn^{+2} + 2e^{-}$	-0.763
$Cr \rightarrow Cr^{+3} + 3e^{-}$	-0.71
$Fe \rightarrow Fe^{+2} + 2e^{-}$	-0.44
$Cd \rightarrow Cd^{+2} + 2e^{-}$	-0.402
$\text{Co} \rightarrow \text{Co}^{+2} + 2e^{-}$	-0.27
$Ni \rightarrow Ni^{+2} + 2e^{-}$	-0.23
$\operatorname{Sn} \to \operatorname{Sn}^{+2} + 2e^{-}$	-0.136
$Ni \rightarrow Ni^{+2} + 2e^{-}$	-0.126
$2H^+ + 2e^- \rightarrow H_2$	0.000 (reference)
$Cu \rightarrow Cu^{+2} + 2e^{-}$	0.34
$2Hg \rightarrow Hg_{2}^{+2} + 2e^{-}$	0.788
$Ag \rightarrow Ag^{+} + e^{-}$	0.799
$Pd \rightarrow Pd^{+2} + 2e^{-}$	0.83
$Pt \rightarrow Pt^{+2} + 2e^{-}$	1.188
$O_{2} + 4H^{+} + 4e^{-} \rightarrow 2H_{2}O$	1.23
$Au \rightarrow Au^{+3} + 3e^{-}$	1.498 (noble)
$Au \rightarrow Au^+ + e^-$	1.692

The resulting electrode potential, the corrosion potential  $E_{\rm corr}$  (also known as the open circuit potential), is a mixed potential at which the rates of dissolution and cathodic

reduction are equal, so that there is no net current. In order to evaluate the corrosion rate (by electrochemical techniques), the electrode potential must be changed in either the anodic or the cathodic direction, the net current measured, and the obtained data extrapolated to the open circuit potential. If the potential is controlled above  $E_{\rm corr}$ , the net current is anodic, approximately equal to the rate of metallic dissolution. Below  $E_{\rm corr}$  the net current is cathodic, close to that expected for the reduction of the oxidizing agent. At the corrosion potential, the two rates are equal to each other and to the corrosion rate. The fact that there is no net current only indicates that the electrons generated by the metallic dissolution are consumed by the cathodic reaction.

The corrosion rate, which is evaluated in terms of the current, can easily be converted into other units with the use of the Faraday law and conversion factors; that is, the number of coulombs of electricity associated with 1 gram-equivalent of any ion is F, equal to 96 493.5 coulombs/equivalent. For example, the corrosion expressed in terms of the rate of the metallic recession L in cm/s can be calculated as

$$L = iM/zF\rho \qquad \{\text{cm/s}\} \tag{7}$$

where the current i is in A/cm<sup>2</sup>, M is the molecular weight in grams, and  $\rho$  is the density in g/cm<sup>3</sup>.

The sensitive dependence of the current on potential can be used either to study reaction kinetics in the laboratory (see below), or to understand many practical consequences of corrosion reactions. The spatial distribution of individual reactions may be random, resulting in a uniform corrosion loss, or it may be governed by surface geometry, morphology, crystallographic or chemical aspects, etc., giving rise to various forms of localized corrosion. In thinfilm structures, the presence of defects such as notches, scratches, seams between metals and dielectrics, grain boundaries, and intermetallic phases all present possibilities for enhanced localized corrosion.

# • Corrosion testing

Testing for corrosion is usually conducted in laboratory and field environments. The methodology existing for the bulk materials is generally applicable to thin films such as those used for forming VLSI interconnections. However, there is a limited amount of metal in a thin film, and its disappearance during a test could lead to misinterpretations. Because of the complexity of corrosion reactions and the many factors which can influence them, tests should be well planned, materials characterized beforehand, and the conditions needed for a functional life of the product well projected. Laboratory tests are normally conducted either in accelerated corrosion chambers or in an electrochemical cell. The aggressiveness of the tests in atmospheric chambers depends on the

temperature used, the relative humidity, and the possible introduction of controlled amounts of pollutants. Tests may be further accelerated by the application of a voltage between two conducting lines. The progress of corrosion can be monitored by resistance change, defect counting and mapping, and numerous surface-sensitive techniques such as ellipsometry, Auger electron spectroscopy (AES), X-ray photoelectron spectroscopy (XPS), or reflectivity, often coupled with functional tests of the samples under examination.

In electrochemical cells, samples are placed in an electrolyte, and their behavior is monitored by electrochemical techniques. In our laboratory several types of custom-made cells are used. One is an airtight three-electrode cell, fabricated from Kel-F material (manufactured by 3M, St. Paul, MN) and equipped with quartz windows. This cell provides the possibility of using solutions saturated with either N, or O, and the capability for simultaneous electrochemical and ellipsometric measurements under well-defined conditions. Another type is a much simpler, miniature cell, designed to duplicate the conditions of atmospheric corrosion. The cell has been described in detail elsewhere [10]. Since it is specially designed for microelectronic corrosion studies, a brief description of the cell is presented here (Figure 3). The cell consists of the sample (working electrode) masked with punched plating tape to expose an area of 0.32 cm<sup>2</sup>, a Pt mesh (counter electrode), a reference electrode, and filter paper disks separating each electrode; it can be used with a 20- $\mu$ l droplet of electrolyte. Because of the small distances between the electrodes, the ohmic resistance in the cell is relatively small, even when use is made of triply distilled water as an electrolyte.

Electrochemical techniques offer a variety of approaches for studying corrosion phenomena. We have utilized dc techniques, such as potentiodynamic polarization and linear polarization. In potentiodynamic polarization the potential is ramped through a fairly wide potential range, both below and above the corrosion potential, revealing the kinetics of both the cathodic and anodic processes, the corrosion rates, the dissolution mechanisms, the ability of the metal being investigated to passivate itself, and an assessment of pitting or possible galvanic exposure. During linear polarization the potential is scanned only within  $\pm 10$ –20 mV of  $E_{\rm corr}$  so that the metal under investigation is barely disturbed by the measurement. The slope of potential vs. current is inversely proportional to the corrosion rate. These measurements are fairly precise and can be carried out rapidly. Use is made of a reference electrode containing a saturated mercurous sulfate solution. The potentials subsequently cited are with respect to such an electrode (MSE), namely, vs. MSE.

A good correlation of electrochemical corrosion measurements and environmental tests has been exhibited by several studies in which a direct comparison of the two methods was carried out [11, 12]. This should not be too surprising because at temperatures at which the water is liquid, in either bulk or thin-film form, the predominating corrosion process is electrochemical; i.e., metallic wastage occurs through anodic dissolution [6]. The physical aspects of water adsorption suggest that the role of water in atmospheric corrosion should not be much different from that expected in a bulk solution [13]. Once the adsorbed water is about three monolayers thick (at about 65% relative humidity), its behavior is similar to the action of a bulk solution; i.e., it acts as a solvent for both metallic ions and corrosive gases [13].

The electrochemical techniques used in the studies described in this paper involved use of the following electrolytes: 1) water; 2) 0.1 N K, SO, with a pH level adjusted to 2 to 14; 3) buffered HF; and 4) Cu etchants such as (NH<sub>4</sub>)<sub>2</sub>S<sub>2</sub>O<sub>8</sub> and Fe(NO<sub>3</sub>)<sub>3</sub>, all with or without inhibitors such as silicates, phosphates, and 1 H-benzotriazole (1 H-BTA). In the case of copper, electrochemical techniques were used both to control the oxidation state of the surface prior to testing and to monitor the corrosion behavior during testing. In many cases native copper oxides were first reduced at a low cathodic potential, after which either the spontaneous reoxidation at the open circuit potential or electrode reactions at some applied potential could be measured. Many experiments were conducted with in situ ellipsometry, which makes it possible to monitor the removal of the native oxides as well as the formation of surface films arising from corrosion or purposeful oxidation. Ex situ surface science techniques, such as XPS, time-of-flight static secondary ion emission spectroscopy (ToFS-SIMS) and high-temperature mass spectroscopy were used to elucidate surface composition. In cases in which the metallic surface had been exposed to reactive ion etching, the surface contaminants were determined by ion chromatography (IC) and inductively coupled plasma (ICP) techniques.

#### • Corrosion of thin-film and bulk samples

In a study of CoCr alloys, thin films were found to corrode at higher rates than bulk alloys [14], although both showed a similar dependence on Cr content. On the other hand, the corrosion rate of Cu measured on films and bulk material tended to be similar. The behavior of thin films, however, can be greatly altered depending on the conditions that applied during film deposition. For example, the thermal activation energy for the corrosion of CoCr films in temperature/humidity (T/H) tests has been found to vary from 0.07 to 0.3 eV, depending on their sputter-deposition conditions [15]. The use of thin-film materials whose properties depend upon deposition parameters leads to further complications in the

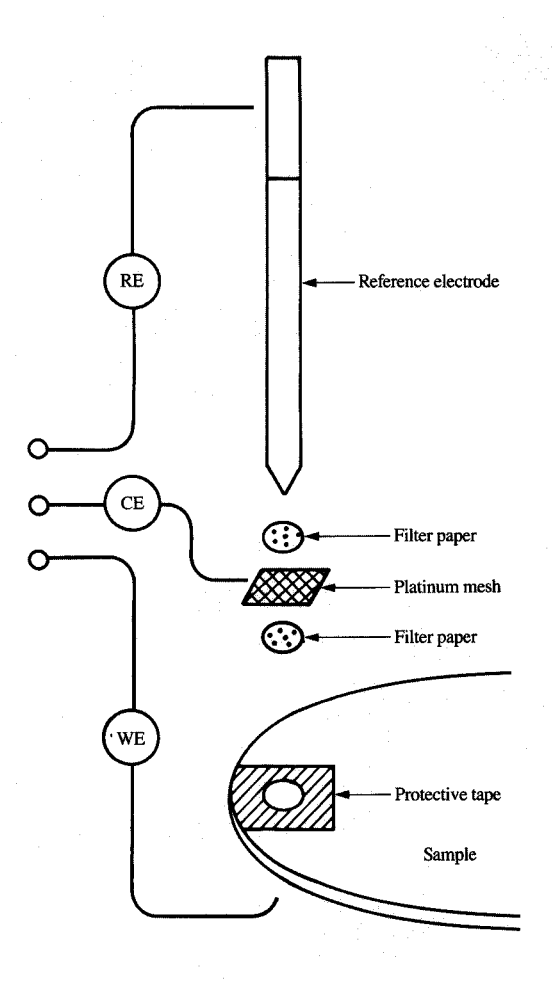


#### Figure 3

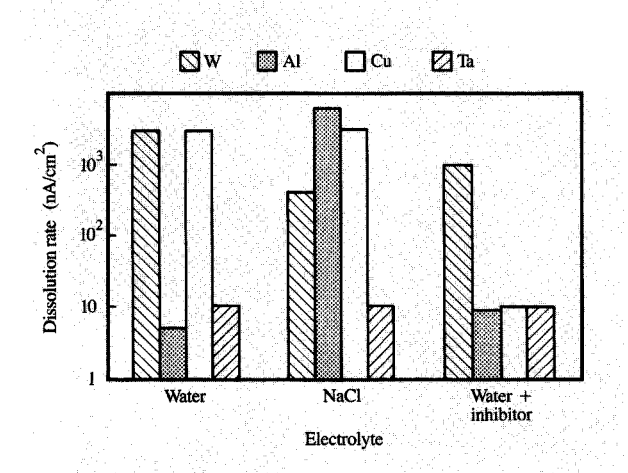
Schematic of cell used for the measurement of corrosion in a droplet of an electrolyte, showing the reference electrode (RE), counter electrode (CE), and working electrode (WE).

optimization of corrosion resistance. Although some properties of pure Al and Cu thin films also depend upon film preparation conditions, there are no reports connecting their preparation conditions with their widely varying corrosion behavior. On the other hand, the corrosion resistance of Al-Cu films depends strongly on parameters such as the size and distribution of Al<sub>2</sub>Cu intermetallics [16] in the films.

## Corrosion in processing

## • Al-Cu and Cu in water

As mentioned above, metallic dissolution is a very sensitive function of the environment. **Figure 4** shows the dissolution rate of as-deposited, native-oxide-covered Al,



Dissolution rates of W, Al, Cu, and Ta in water, 0.1% NaCl, and water containing an inhibitor (1*H*-BTA).

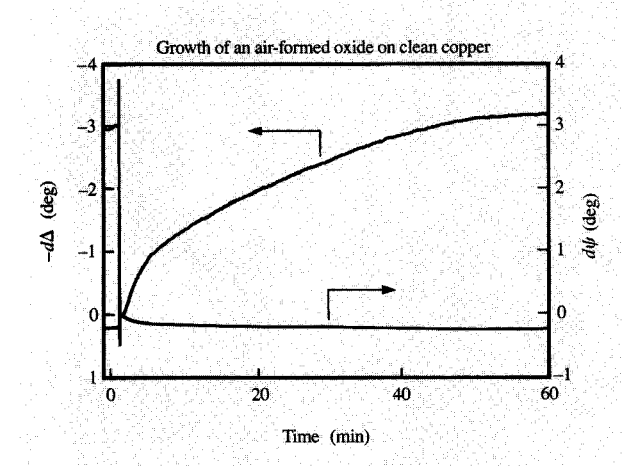


# Figure 5

Ellipsometric data for spontaneous oxidation of Cu in air, starting with an oxide-free surface.

Cu, W, and Ta in relatively mild environments. In air-saturated water, Al and Ta are protected by native oxides, i.e., are passive, while Cu and W show a considerable susceptibility to corrosion. In air-saturated water with the presence of chlorides ( $\approx 1000$  ppm), Ta remains corrosion-resistant, Al loses its passivity and shows localized corrosion, W becomes more resistant due to the formation

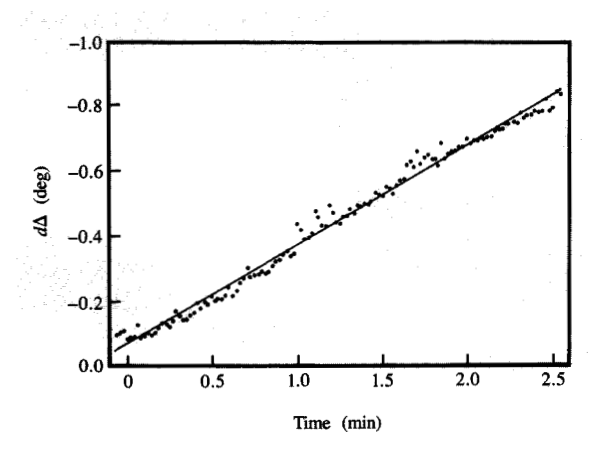
of oxy-chloro-complexes, and Cu dissolution remains unchanged. However, in water containing  $10^{-2}$  M benzotriazole (1 *H*-BTA), the corrosion of Cu becomes as low as that of the passive Ta or Al.

It is possible in some cases to influence corrosion resistance and provide viable means for corrosion control. Figure 4 also indicates several differences between Cu and Al. Aluminum is thermodynamically reactive but kinetically passive. The behavior of Al (actually its very existence) is governed by the stability of its oxide film. The oxide forms very readily, grows in a self-limiting fashion, and is very protective in many environments of practical importance. The data indicate that the average corrosion rate of Al in water is less than 0.0002 nm/min. While Cu is more noble, its oxide is not particularly passive, and its corrosion rate in the presence of dissolved oxygen is much higher than that of Al. i.e., about 0.1 nm/min. On the other hand, the corrosion rate of Cu can be reduced by the use of inhibitors. No similarly effective inhibitors exist for aluminum in neutral environments at room temperature.

• Native oxides on Cu and Al and corrosion testing
Copper is readily prepared in an oxide-free state. For
corrosion studies, an oxide-free surface can be prepared by
exposure to a slightly acidic environment (e.g., dilute
sulfuric acid with a pH of 4) for a few seconds or simply
by cathodic reduction in almost any electrolyte. Thus, the
corrosion of Cu can be studied in a controlled fashion in a
chosen environment both in the oxide-free and oxidecovered state.

Ellipsometric analysis of a reduced Cu surface in solution was found to result in a well-defined complex index of refraction of the clean Cu surface, namely 0.23691-3.6539i. With these data we could calculate the ellipsometric parameters  $\Delta$  and  $\psi$  to be 112.5 and 43.38°, respectively, which an oxide-free Cu surface should display in air if that state were attainable. An experimental attempt to measure such values was successful. A Cu thin film deposited onto a Si substrate was affixed to the sample holder of an ellipsometric table, spray-washed with a pH 4 sulfuric acid solution, and continuously dried with a clean nitrogen jet. Ellipsometric measurements were noisy but resulted in  $\Delta$  and  $\psi$  values within half a degree of the calculated values. However, the oxide-free state of the surface was not long-lived. As soon as the sulfuric wash was stopped, reoxidation of the surface began. The ellipsometric changes that resulted from the oxide growth are shown in Figures 5 and 6. As the oxide thickness increases,  $\Delta$  and  $\psi$  decrease, which is expected for a thin, absorbing film. While the film remains thin, the change in  $\Delta$  is a linear function of the change in oxide thickness, with a one-degree change in  $\Delta$  being equal to an increase in oxide thickness of about 0.5 nm.

The oxide growth in room air at a relative humidity of ≤50% was followed for 72 hours, with the changes obtained within the first hour shown in Figure 5. As indicated in Figure 6, the oxide appeared to grow linearly with time t during the first two minutes of growth (corresponding to an oxide thickness of 0.5 nm) and as  $t^{1/3}$ subsequently. After about an hour, the oxide thickness reached about 1.5 nm, and after 72 hours about 3.5 nm. The linear-to-cubic transition is well-documented for higher temperature [17]. The data indicated that the reaction of thin Cu films at room temperature in relative humidity ≤50% follows the same rate laws. The oxide growth mechanism responsible for the observed thickness-time relation is best described by the combining of Cu ions and oxygen at the outer oxide/air interface, with the ratedetermining step being the diffusion of Cu ions via Cu-ion vacancies, the distribution of which decreases linearly with oxide thickness [17].



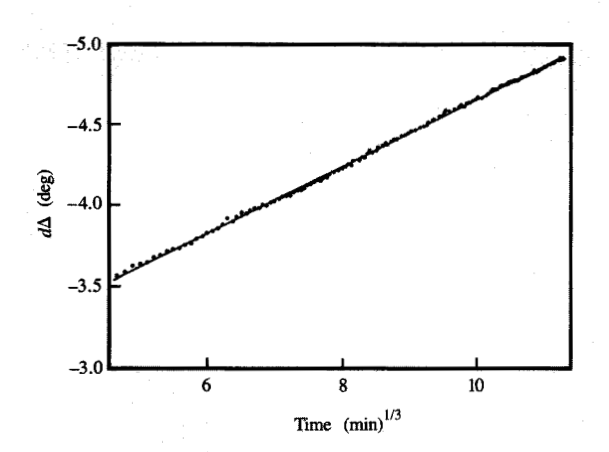
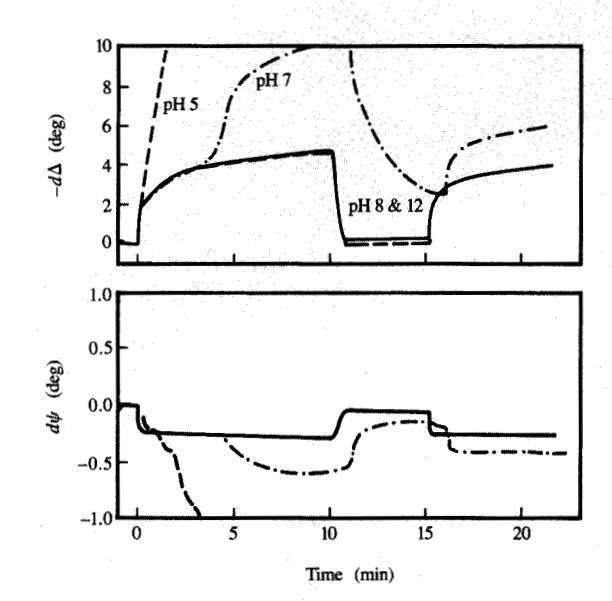


Figure 6.

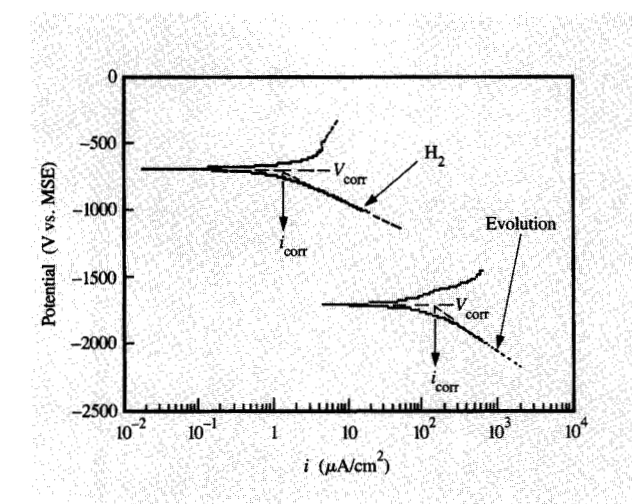
Linear (initially) and cubic (subsequently) behavior for air oxidation of Cu at room temperature.



# Figure 7

Spontaneous oxidation of Cu in air-saturated  $0.1\,\mathrm{N}~\mathrm{K}_2\mathrm{SO}_4$ , at pH levels of 5, 7, 8, and 12. Portions of the figure from [25], reprinted by permission of the publisher, The Electrochemical Society, Inc.

Reoxidation of an oxide-free Cu surface also occurs quickly and spontaneously at open circuit in many airsaturated electrolytes. Ellipsometric data are shown in Figure 7 for copper in 0.1 N K, SO, at pH levels of 5, 7, 8, and 12. In all cases the native oxides were initially reduced at the cathodic potential of -1.6 V. When the potential control was removed at time zero, the Cu was readily reoxidized in a solution having a pH level in the range of 8-12, with the oxide growth being logarithmic, as was visible from the relative change of ellipsometric parameters, notably  $d\Delta$ . The change of  $\psi$ , corresponding to the oxide growth, was about one tenth of the change measured in  $\Delta$ , as expected for the well-behaved oxide film. The oxide could be reversibly reduced by applying a low cathodic potential. The reduction at -1.6 V, applied after about 10 minutes, reestablished the optical value of the oxide-free Cu surface. This process could be repeated reversibly with no significant differences in the optical properties of the oxidized or reduced Cu, indicating that surface roughening did not interfere with the measurement. At a pH level of 7, the initial stages of oxide growth were similar to those in more alkaline solutions. In neutral solutions, however, the oxide is not a perfect corrosion barrier and can be undermined by continuous dissolution. Consequently there was an abrupt and irreversible change



Potentiodynamic polarization curves for Al-4%Cu, obtained during contact with scouring pad (lower curve) and about 5 min after removal of the pad.

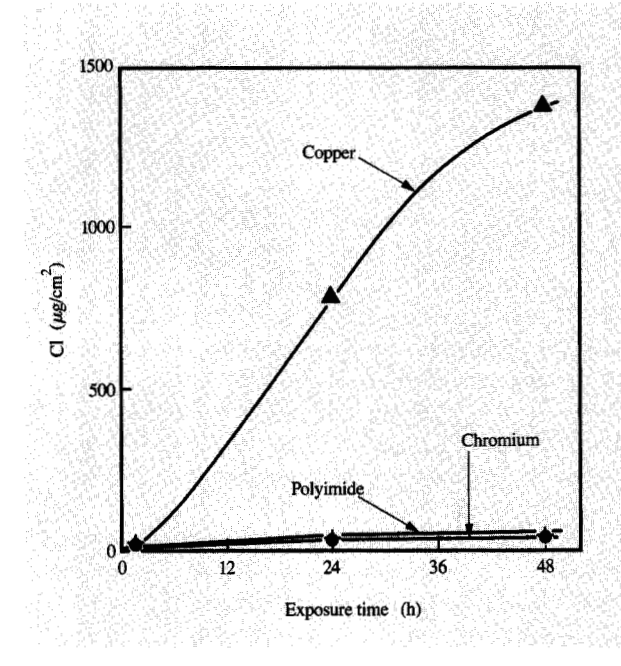


# Figure 9

Amount of chloride detected on copper (upper curve), chromium, and polyimide (lower curves), after an atmospheric corrosion test at room temperature, in 70% relative humidity and 12 ppb of Cl<sub>2</sub>.

in the measured data, which appeared to be caused by surface roughening. At lower pH levels, e.g., a pH level of

5, dissolution prevailed, and the ellipsometric change was entirely due to surface roughening, with particularly large changes in  $\psi$ .

While copper is found in nature as an element and has been used for more than 10 000 years [18], aluminum is found only in compound form and has been prepared for practical use only recently [19]. Because Al oxide cannot be electrochemically reduced, we did not study the formation of Al oxide on oxide-free Al. Others have suggested that Al at ambient temperature forms an oxide by a logarithmic growth law [20, 21]. Such growth is thought to be limited by field-assisted ionic migration through the oxide, which is slower than the movement by diffusion, suggesting a higher resistance for ionic movement and better protection against corrosion.

Once an oxide has formed on an Al surface, it is possible to dissolve it in a strong alkali, but such an approach results in surface roughening and is not applicable to the behavior of an oxide-free Al surface in other solutions. A better approach is to remove the oxide by in situ abrasion. Experiments were performed with an Al-4%Cu rod, imbedded in Teflon using a rotating disk arrangement. The oxide was removed by pressing a scouring pad against the electrode in solution. Simultaneous acquisition of electrochemical data was thus possible. After measurements with abrasion, the rod was raised, and measurements were repeated without abrasion but with the same rotation rate. Although we did not have direct evidence of the oxide growth, electrochemical data that were obtained showed that the surface quickly became repassivated, as indicated in Figure 8. Five minutes after the cessation of scouring, the measured corrosion rate decreased by two orders of magnitude.

In summary, since all metals (except gold) spontaneously oxidize in air, many corrosion tests simply reflect the stability of the native oxide in a given environment unless specific steps are taken to remove the oxide. It is important to keep this in mind when interpreting corrosion data.

# • Effects of chlorides

The presence of chlorides significantly increases the corrosion rate of aluminum, as indicated in Figure 4, by causing a local breakdown in the protective oxide with associated pitting. Some details of the mechanism by which the attack occurs are discussed below. The effect of chlorides on the corrosion of Cu is barely measurable in electrochemical tests (Figure 4), but its corrosion becomes very noticeable in a humid atmosphere containing chlorine or hydrochloric acid. The difference could be attributed to 1) the fact that Cu oxide is poorly protective in neutral solutions, accounting for the observation of relatively high corrosion rates even in pure water and 2) the significantly lower surface pH level that was attained in the atmospheric corrosion chamber. When Cu was placed

in a corrosion chamber containing 70% relative humidity and 12 ppb of Cl<sub>2</sub> at 25°C, the diffusion-limited growth of natural oxides was replaced by a fast, almost linear, growth of corrosion products. Ellipsometry indicated that within 48 hours the product thickness exceeded 100 nm. Thus, the chlorides cause a significant acceleration of corrosion rate. The primary composition of the corrosion product is CuCl<sub>2</sub>. This is judged by the fact that the surface contains large amounts of soluble chlorides, which are detectable by IC, and that CuCl is insoluble. In contrast, the solubility of CuCl<sub>2</sub> is high, i.e., 70.6 g per 100 ml of water. The amount of adsorbed chlorides on an inert surface such as chromium or polyimide is significantly lower, i.e., below 40 ng/cm<sup>2</sup>, as can be seen in **Figure 9**.

• Effects of pH on dissolution of Al, Al-Cu, and Cu The effect of pH on Cu corrosion, shown in Figure 10, may be viewed as an extension of Figure 7. In water and neutral electrolytes, Cu oxides are stable. Oxygen reduction is the primary cathodic reaction and is diffusioncontrolled. Oxygen reduction is also responsible for the dissolution of Cu at pH levels of 12 and 2, yet the corrosion rate is clearly higher in an acidic solution and much lower in an alkaline one. The explanation for the difference is given by the state of the copper surface; there is a native oxide present at a pH level of 7, additional oxide growth in alkaline solutions, and no oxide in acidic solutions. Only in acidic solutions does the rate of oxygen diffusion reach the limiting current density of  $5 \times 10^{-}$ A/cm<sup>2</sup>, which is expected for the amount of dissolved oxygen in solution [6]. At higher pH levels, at which Cu oxides are not spontaneously dissolved, a good part of the reactive sites are no longer available for reaction; thus, the corrosion rate is somewhat lower. However, copper dissolution occurs readily even at a neutral pH level, with the anodic Tafel slope close to 40 mV/decade (Figure 10). The slope of 40-60 mV/decade has also been reported by others [22] for dissolution from oxide-free Cu in acidic solutions. It seems that Cu oxide in neutral electrolytes affects the rate of Cu dissolution without changing the mechanism, as if only partially blocking the surface. From the corrosion viewpoint, the low anodic Tafel slope is an indication of the lack of protection by the surface oxide. Copper is relatively passive only in alkaline solutions, as indicated by a reduction of the corrosion rate and an increase of the Tafel slope. This indicates a change in anodic dissolution mechanism: The activation energy for the exodus of Cu ions increases, and the dissolution process involves an ion migration through the oxide.

The corrosion rate of Cu measured at pH levels of 2–14 is shown in **Figure 11**, indicating that the lowest rate occurs in the pH range from 7 to 12, where the oxide is the most stable. The addition of 1 *H*-BTA to each of the electrolytes causes a significant decrease of the corrosion

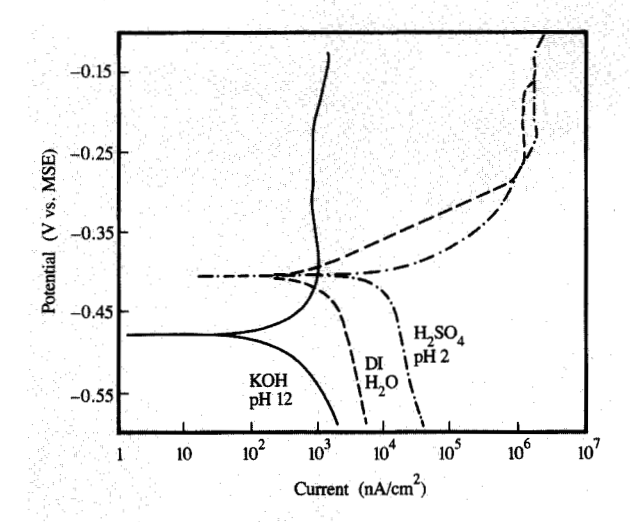


# Figure 10

Potentiodynamic polarization curves measured on Cu at pH levels of 2, 7.3, and 12.

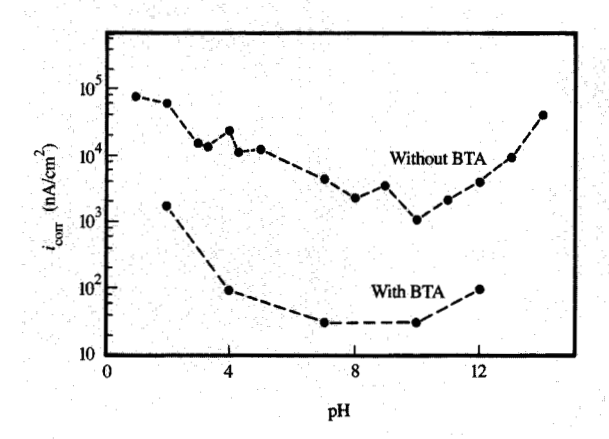
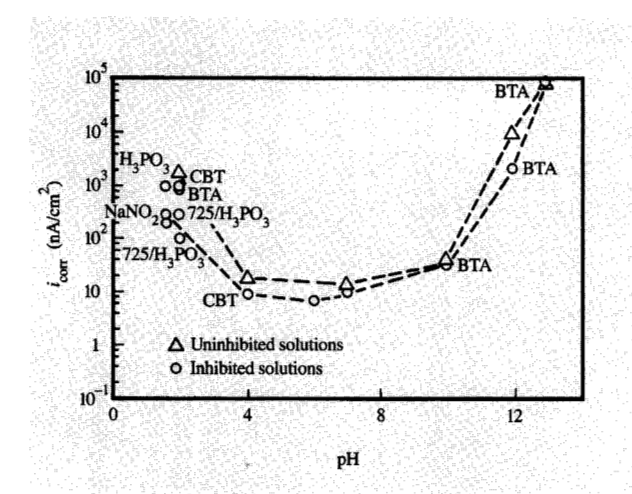


## Figure 11

Corrosion rate of Cu as a function of pH level in  $0.1\,N~K_2SO_4$ , with and without benzotriazole present. Portions of the figure from [25], reprinted by permission of the publisher, The Electrochemical Society, Inc.

rate. The nature and effectiveness of the new surface film, Cu-BTA, has been the subject of a large body of work, since 1 *H*-BTA was first used as an inhibitor for Cu corrosion [22–25]. Depending on the preparation



Corrosion rate of Al-Cu films as a function of pH in  $0.1\,\mathrm{N}\ \mathrm{K}_2\mathrm{SO}_4$ , with and without inhibitors present.

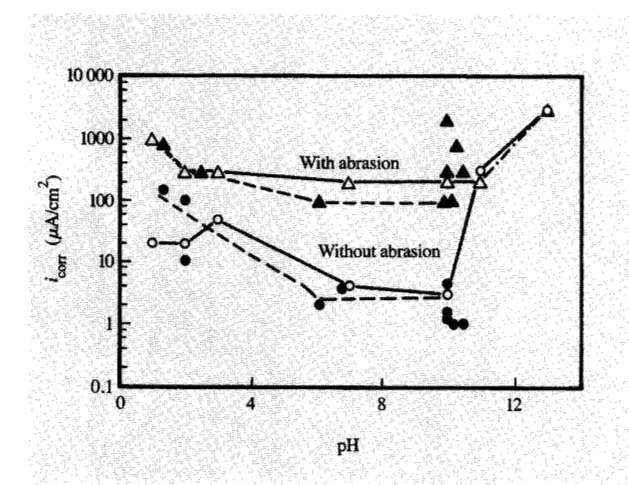


# Figure 13

Corrosion rate of Al, with or without abrasion, at different pH levels, with and without inhibitors present (dashed and solid lines, respectively).

conditions, Cu-BTA films can grow in ten minutes to a thickness of 2–26 nm, with the thinnest films formed at neutral and alkaline pH levels being the most polymerized and the most protective against corrosion [25].

In comparison with Cu, an Al-Cu film shows a significantly lower corrosion rate over a broad pH range (using  $0.1 \text{ N K}_2\text{SO}_4$  as a supporting electrolyte), except in very acidic (pH 2) and alkaline (pH > 11) solutions, in

which the aluminum oxide dissolves (Figure 12). Although inhibitors, such as 1 *H*-BTA and its derivatives, a chromate, a phosphate, a silicate, and a nitrite, have been reported to be effective for Al [26, 27], our results have shown that they have very little effect on the corrosion rate. Over the broad pH range in which corrosion is low because of protection by the native oxide, one could argue that the benefits of the inhibitors are not measurable. A more sensitive measurement has been carried out using the rotating aluminum rod/scouring pad approach discussed above. The data, obtained from the measurements shown in Figure 8, are summarized in Figure 13, and show that the results of self-passivation obtained with inhibitors present yielded a small improvement (by a factor of 2–5) in comparison to those obtained in the absence of inhibitors.

Corrosion of Al-Cu and Cu exposed to reactive ion etching

#### Al-Cu

Interconnections for VLSI circuit chips are most commonly fabricated with Al-Cu alloy (containing several % Cu) thin-film lines patterned by reactive ion etching [7, 28, 29]. Pattern definition of the Al-Cu by a Clcontaining plasma leaves the wafer surface and photoresist (masking) layer contaminated with chlorides. Subsequent steps must be as well controlled as the etching process itself, because corrosion of the etched Al-Cu occurs to varying degrees as soon as the freshly etched film is exposed to air. Depending on the environment, the loss of the conductor can be catastrophic. From the moment the film is exposed to the humidity contained in a laboratory, manufacturing, or storage environment, the principal etch product retained or redeposited onto the walls, AlCl,, can hydrolyze, and the formation of a healthy oxide may be replaced with the growth of voluminous, unprotective corrosion products [30, 31], typically

$$AlCl_3 + 3H_2O \rightarrow Al(OH)_3 + 3HCl_4$$
 (8)

$$Al(OH)_3 + 3HCl + 3H_2O \rightarrow AlCl_3 6H_2O, \tag{9}$$

and

$$2(AICl_3 6H_2O) \rightarrow Al_2O_3 + 9H_2O + 6HCl.$$
 (10)

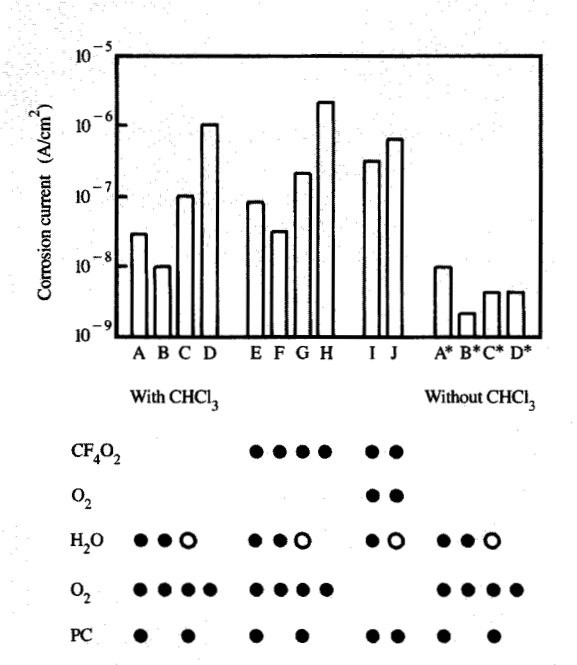
The chloride ions, freed by the hydrolysis of original chloride compounds, can attack the poorly passivated aluminum and continue a cycle of continuous, accelerated corrosion [31, 32], namely

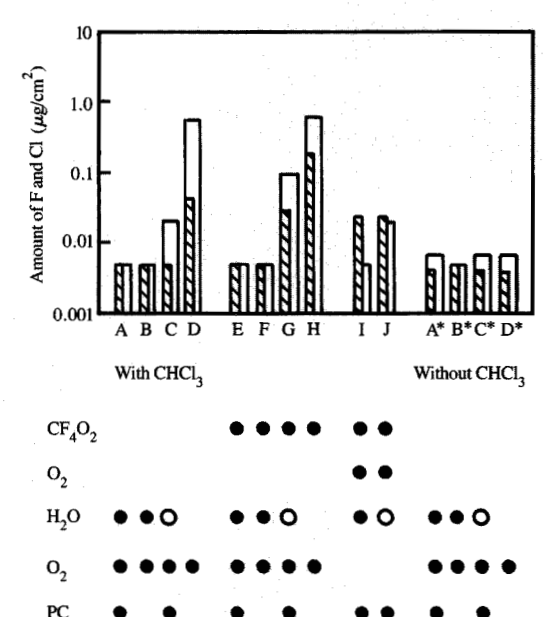
$$Al + 4Cl^{-} \rightarrow AlCl_{4}^{-} + 3e^{-}$$
 (11)

and

$$AlCl_{4}^{-} + 3H_{2}O \rightarrow Al(OH)_{3} + 3H^{+} + 4Cl^{-}.$$
 (12)

The problem is aggravated by the fact that the reactive ion etching (RIE) results in a surface decorated with Cu-





Corrosion rate of Al-Cu in water droplet (left) and the amount of halides on the surface (right) as a function of RIE and post-RIE cleaning steps. The circles indicate the cleaning step used; those that are designated by open circles involved use of a 30-min delay in a water wash. Samples designated with asterisks were processed without CHCl<sub>3</sub> present during the last RIE step. The amounts of chloride detected are noted by the open bars and the amounts of fluoride by the shaded ones. From [33], reprinted by permission of the original publisher and copyright holder, the National Association of Corrosion Engineers.

rich residues which galvanically enhance localized corrosion of the aluminum matrix of the Al-Cu. We have detected chloride on the etched surface, particularly on the Cu-rich intermetallic phase, by AES and XPS, and we have studied the effects of RIE and post-RIE cleaning steps on Al-Cu corrosion. The results are reported in [33], and are briefly summarized here.

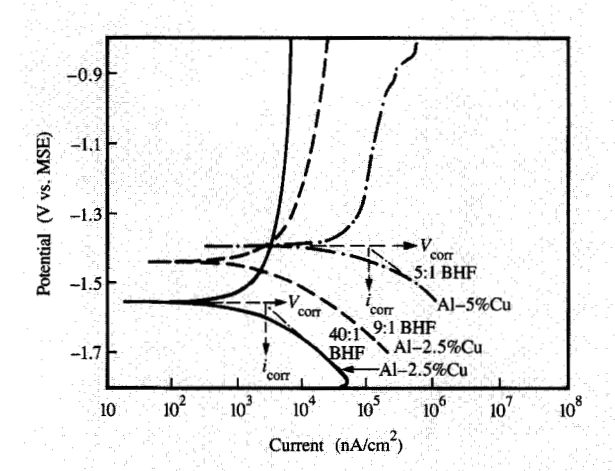
The samples used were prepared under broadly varied but controlled conditions, in a form amenable to analysis by electrochemical tests—in a droplet of triply distilled water added to the surface. The water dissolves soluble residual contamination to produce an environment, the aggressiveness of which depends on the extent of the contamination. The electrochemical data were correlated with residual surface impurities, which were quantitatively determined by IC and ICP. The results, illustrated in Figure 14, showed an excellent correlation of the corrosion rate and residual halide content, and indicated that the most effective halide cleaning sequence is an immediate water rinse, followed by photoresist stripping (in O<sub>2</sub> plasma) and etching with a chromic–phosphoric acid

mixture, clearly confirming results published earlier [34, 35]. Post-RIE cleaning steps were thus shown to be crucial for the survival of the Al–Cu metallization during process steps preceding the application of a more lasting type of protection, obtained through the use of an overlying sputtered SiO, layer.

#### Copper

The low volatility of Cu<sub>2</sub>Cl<sub>2</sub> makes the RIE of Cu conductors difficult to accomplish, although there have been several successful attempts reported [36–38] which involved the use of an elevated wafer temperature and, possibly, energetic ion bombardment. Schwartz and Schaible [36] have reported that no corrosion was observed after RIE of masked Cu in CCl<sub>4</sub>/Ar plasmas using high power and a heated cathode (225°C). The wafers were hot when removed from the RIE reactor and were immediately rinsed in deionized (DI) water. We have investigated the behavior of unmasked Cu in water after

<sup>&</sup>lt;sup>1</sup> G. C. Schwartz and P. M. Schaible, IBM East Fishkill facility, Hopewell Junction, NY, private communication.



Potentiodynamic polarization curves for Al-5%Cu films in BHF having a 5:1  $NH_4F/HF$  ratio, and for Al-2.5%Cu in 9:1 and 40:1 BHF.

Table 2 Corrosion in a water droplet of Cu exposed to RIE

Sample	Treatment		Potential (V vs. VSE)	Corrosion	
	$\frac{BCl_3/Cl_2}{10~\rm s}$	<i>CF</i> ₄ 20 s	$H_2O$	(V VS. VSE)	rate (A/cm <sup>2</sup> )
1	yes	no	по	-0.37	$9 \times 10^{-5}$
	yes	no	yes	-0.37	$8 \times 10^{-5}$
2 3	yes	yes	no	-0.37	$2 \times 10^{-4}$
4	yes	yes	yes	-0.39	$8 \times 10^{-5}$
		120 s			
5	no	yes	no	-0.37	$8 \times 10^{-6}$
6	no	yes	yes	-0.37	$8 \times 10^{-6}$
7	no	yes	no	-0.37	$8 \times 10^{-6}$

exposure to several other types of plasmas, such as BCl<sub>3</sub>/Cl<sub>2</sub> and CF<sub>4</sub> plasmas, without cathode heating and with or without rinsing in water. The exposure to a Cl plasma resulted in noticeable corrosion. The differences may have been due to one of the following possibilities:

1) after RIE patterning the Cu films were heated and rinsed while hot; 2) the sidewalls (unlike the unprotected blanket surface) of the patterned films were subjected to only negligible ion bombardment; or 3) the sidewalls were additionally protected by a polymer film derived from the CCl<sub>4</sub>. The results of the investigation are listed in **Table 2**.

Exposure of a Cu film to a BCl<sub>3</sub>/Cl<sub>2</sub> plasma leads to catastrophic corrosion, with a rapid deterioration of its surface (Sample 1). The corrosion product formed in

seconds cannot be removed by a water wash (Sample 2) or a subsequent exposure to a CF<sub>4</sub> plasma (Sample 3). The corrosion rate of those samples, measured in a droplet of water, was found to be at least ten times higher than for as-deposited Cu films and displayed no hindrance to the oxygen reduction reaction.

In contrast, the use of a CF<sub>4</sub> plasma was not found to be aggressive to the copper surface. The surface remained bright, covered only by about 10 nm of the new surface film, as detected by ellipsometry. XPS surface analysis revealed primarily CuF<sub>2</sub> and some oxide. The corrosion rates in water, with or without rinsing in water, were found to be similar to rates measured on control films that had not been exposed to a CF<sub>4</sub> plasma.

#### • Al-Cu and buffered HF

During the formation of VLSI circuit interconnections, patterned Al-Cu layers are usually coated with insulating layers, most often consisting of SiO,, deposited by sputtering or plasma-enhanced chemical vapor deposition (PECVD). The use of RIE in an F-containing plasma has almost universally supplanted the use of buffered HF (BHF) for etching the SiO, to form the through (via) holes used to interconnect the Al-Cu (or Al-Cu-based) layers in the multilevel structures. However, the wafer Al-Cu layers are sometimes also exposed to BHF [followed by a rinse in deionized (DI) water] for the removal of processing residues. Several effects of exposing Al-Cu films to BHF/DI water have been examined: dissolution of such films upon contact with BHF, their active-passive behavior in dilute BHF (as applicable to rinsing) and possible galvanic effects in the multilevel structures (because of possible contact with other dissimilar metals). We have emphasized Al-Cu because it has been the conductor of choice for VLSI for many years.

# • Dissolution of Al-Cu in BHF

Potentiodynamic polarization curves for two Al-Cu films immersed in different BHF solutions are shown in **Figure 15**. The results showed that the corrosion potential decreases with an increase in pH level (i.e., an increase in NH<sub>4</sub>F/HF ratio), but in all cases it is low. The average corrosion rate in BHF with, for example, a 9:1 NH<sub>4</sub>F/HF ratio was found to be less than 0.1 nm/min. There was no active potential region, and the current seemed to be limited by the presence of a surface film. The composition of the film evaluated with XPS (after an extensive rinsing with water) was found to be predominantly Al oxide with a small amount of Al fluoride present. <sup>3</sup> One could speculate, however, that during the exposure to BHF this film

<sup>&</sup>lt;sup>2</sup> S. Cohen, IBM Thomas J. Watson Research Center, Yorktown Heights, NY,

R. Flitsch, IBM East Fishkill facility, Hopewell Junction, NY, private communication.

contained more of the poorly soluble hydrated aluminum fluoride, possibly formed by a dissolution-precipitation mechanism. The film is apparently quite protective, so that the anodic current (or aluminum dissolution rate) stays relatively low and almost independent of potential, even at more than 0.5 V above the corrosion potential. The cathodic reaction, a counterpart of Al dissolution, consists of hydrogen evolution. The cathodic Tafel slope is about 120 mV/decade, which is typical for hydrogen [1]. The hydrogen evolution rate decreases with pH, as expected. The somewhat disproportionately higher rates of both reactions in 5:1 (NH,F/HF) solution are most likely caused by the presence of somewhat variable amounts of Cu in the Al-Cu films. Since Cu has higher catalytic activity for hydrogen and is more noble than Al, it tends to cause local galvanic attack.

#### • Effects of BHF/water ratio on Al dissolution

The effect of water rinsing was simulated by determining the behavior of Al-Cu films in solutions of BHF having a constant NH,F/HF ratio but with additions of increasing amounts of H,O, i.e., in the ratio from 1:1, 5:1, 10:1, 50:1, 100:1, and 500:1 to infinity (in water alone). The results showed that the films dissolved with a limited, relatively low rate in BHF as mentioned above, but became active and dissolved more rapidly in dilute BHF. This is shown in Figure 16, which compares the measured dissolution of films containing 2.5 wt. % Cu in 9:1 BHF, with and without added water. The environments with added water were impoverished of fluoride, and protection by aluminum fluoride was not achieved. However, they were aggressive enough to diminish the protectiveness of the native oxides. The anodic behavior changed from the one with limited dissolution rates (in BHF) to one characterized by large anodic currents (in diluted BHF). The vulnerability was highest for the solutions diluted with 5 and 10 parts of water. With higher dilution ratios, the Al-Cu films tended to be passive because of the action of their surface oxide. Similar observations were reported previously.4 The results indicated that Al-Cu corrosion is faster in rinsing than in BHF alone, indicating that these steps should be practiced with careful process control.

## Galvanic effects and Al dissolution

The shape of the anodic current-potential curves indicated that galvanic enhancement of aluminum dissolution in BHF should be small; the anodic current remained practically unchanged over a broad potential range. Possible causes of the galvanic attack could have been contact with PtSi, Cu, Cr, or Ti (i.e., some of the many metals and alloys which have a more positive corrosion potential than Al). Data obtained for PtSi films in the same solution indicated that

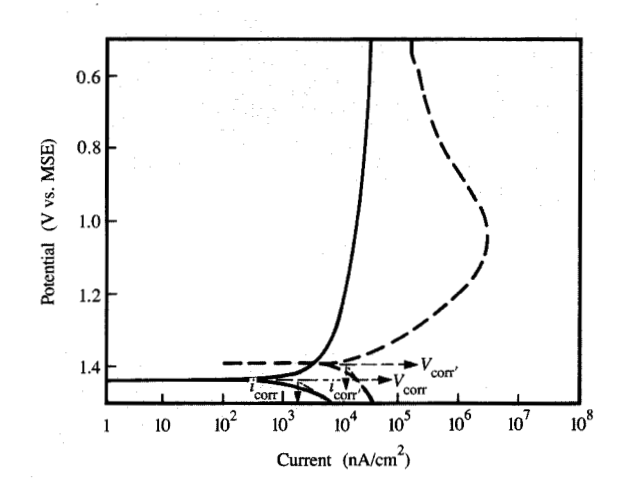


# Figure 16

Potentiodynamic polarization curves for Al-2.5%Cu films in 9:1 BHF, undiluted (solid line) and diluted with 10 parts of water (dashed line, primed values).

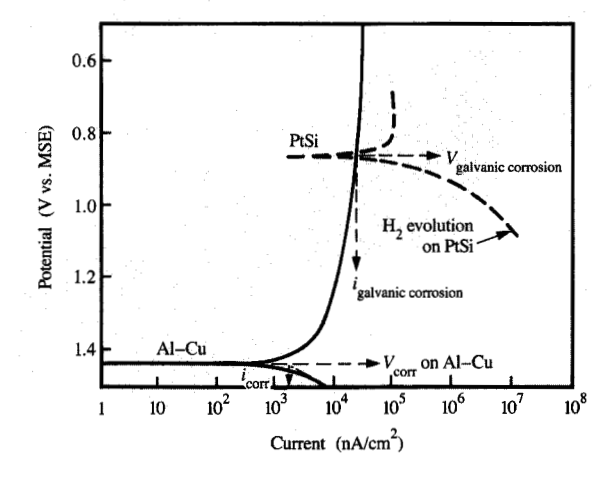
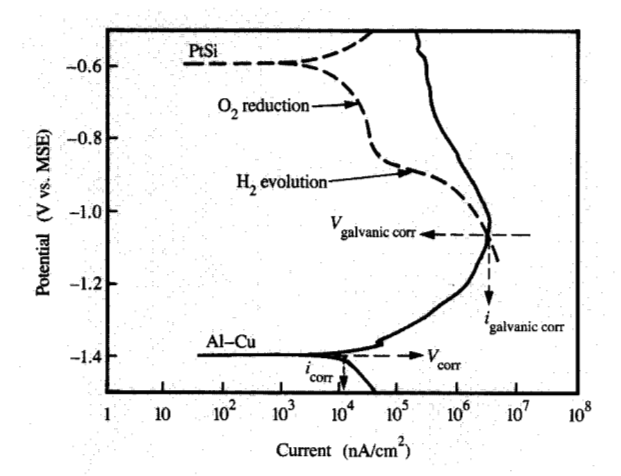


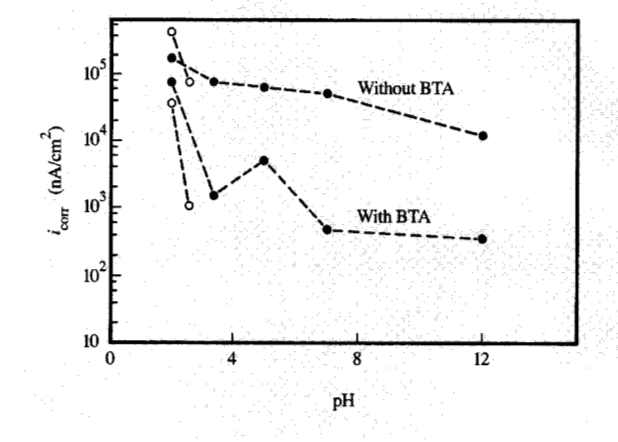
#### Figure 17

Potentiodynamic polarization curve for Al-2.5%Cu and PtSi films in 9:1 BHF.

the galvanic current caused by contact of Al-Cu films with the same area of the PtSi was about ten times higher than the normal corrosion rate (Figure 17). Such a galvanic contact would also result in a galvanic potential which is considerably higher than the corrosion potential. Raising

<sup>4</sup> M. W. MacIntyre, IBM Burlington facility, Essex Junction, VT, unpublished work.





Potentiodynamic polarization curve for Al-2.5%Cu and PtSi films in dilute BHF (9:1), with a water/BHF ratio of 10/1.

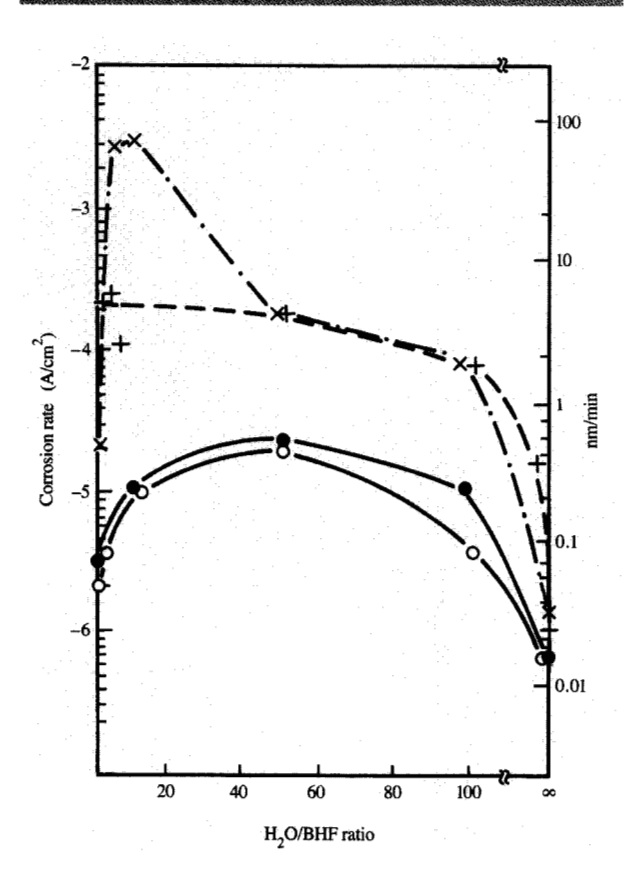


#### Figure 19

Corrosion rate (solid lines) and galvanic corrosion rate (dashed lines) between Al-2.5%Cu and PtSi films of the same area, as a function of BHF and water/BHF ratios: 9:1 BHF ( $\bullet$ ,  $\times$ ); 40:1 BHF ( $\circ$ , +).

# Figure 20

Dissolution rate of Cu films in  $Fe(NO_3)_3$ , and  $(NH_4)_2S_2O_8$  at different pH levels, with and without benzotriazole present. Portions of the figure from [25], reprinted by permission of the publisher, The Electrochemical Society, Inc.

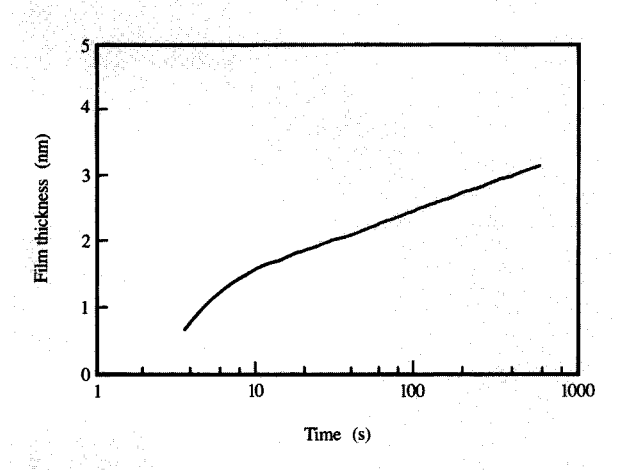
the potential of aluminum could promote metastable pitting, which, however, was not observed in the measured anodic curves. With dilution, both the corrosion rate and in particular the galvanic corrosion rate increased, with the galvanic corrosion rate reaching the very high magnitude of close to 100 nm/min (Figures 18 and 19). The higher the fluoride concentration (40:1 BHF compared to 9:1 BHF), the smaller were the active current and the galvanic current (Figure 19).

# • Cu in etchants

Cu dissolution in suitable etchants can proceed at formidable rates (several tens to hundreds of nm/min). The use of an inhibitor such as 1 H-BTA can not only slow and control Cu removal during etching if needed, but also provide more permanent protection to Cu films during storage between process steps. Some recent data on the interaction between Cu films and 1 H-BTA are summarized in [25]. Figure 20 shows that even in aggressive environments a protective film forms, slowing the etching rate by about two orders of magnitude. The growth of the Cu-BTA films, as studied by ellipsometry, was found to be essentially the same as in simple electrolytes without etchants present. At alkaline pH levels, the growth of the protective film was logarithmic, becoming parabolic growth at lower pH levels, e.g., at 3.4, as indicated in Figure 21. At pH levels below 3.4, the Cu-BTA growth became less reproducible and could best be described by a dissolution-precipitation mechanism. The protectiveness of such films in solutions with inhibitors or in water after

formation reflected their structure and growth. The thinnest films, characterized by logarithmic growth, were the most polymerized (as detected by ToFS-SIMS) and the most protective. It is interesting to note, however, that even the films formed at a pH level of 2 under very aggressive conditions survived water rinsing and provided significant protection in ambient storage.

Differences in the growth of the corrosion product were evident from temperature/humidity testing (Figure 22). The Cu-BTA film reduced corrosion to an extent which depended, as usual, on the environment. It is possible that the Cu-BTA film changes the hydrophilic character of the surface of a Cu film by being an effective barrier for surface wetting [39]. Once the surface is wetted, after some transition time which depends on the environment to which it is exposed, corrosion proceeds at a rate similar to that observed in the absence of the film. This has also



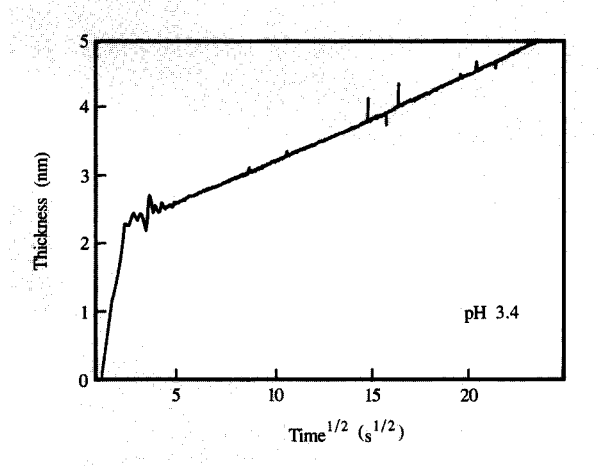
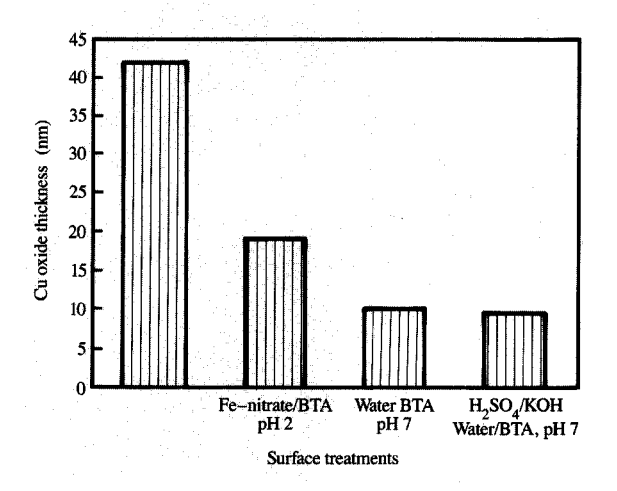


Figure 21

Cu-BTA growth during etching at pH levels of 12 and 3.4.



# Figure 22

Oxide thickness on a Cu film after 14 days of testing at a temperature of 80°C and humidity of 85%. Results are shown for a sputtered Cu film with and without Cu-BTA surface layers present.

been reported by others. <sup>5</sup> Such a delay, however, is quite acceptable in many practical applications for protecting Cu films between processing steps.

# Final remarks

Historically, many methods have been developed to reduce corrosion. However, in the application of such methods to microelectronic circuits, they must be used with care, because restrictions on thin-film dimensions leave little room for corrosion loss. Corrosion can be minimized by the proper choice of materials and environment. As the dimensions of thin-film conductors shrink, their conductivity becomes of increasing concern. The conductivity of the metals of interest decreases in the following order: Ag > Cu > Au > Al > Al-Cu. Therefore, there are only a few good candidates to replace Al-Cu. From the standpoint of corrosion resistance, the best replacement would be Au. Additionally, if combinations of metals are to be used, they should be galvanically compatible and their processing should be optimized to control material loss. After circuit fabrication, reduction of the aggressive nature of the environment to which they are to be exposed should be possible by maintaining its relative humidity below 30%, using inhibitors, or encapsulating the metals with suitable inorganic or organic layers. In the optimization of relevant processing steps, electrochemical techniques should continue to provide useful information on applicable material/environment interactions.

<sup>&</sup>lt;sup>5</sup> R. Sorensen, Sandia Laboratories, Albuquerque, NM, private communication.

# **Acknowledgments**

The authors wish to thank B. Rush, M. A. Frisch, B. N. Eldridge, C. Jahnes, R. Thomas, and D. Pearson for their contributions to this work.

#### References

- 1. M. Pourbaix, Atlas of Electrochemical Equilibria in Aqueous Solutions, Pergamon Press, New York, 1966.
- 2. J. M. West, Electrodeposition and Corrosion Processes, D. Van Nostrand Co., London, 1965.
- 3. C. Wagner and W. Traud, Z. Electrochem. 44, 391 (1938).
- 4. G. Kortum and J. O'M. Bockris, Textbook of Electrochemistry, Elsevier, New York, 1951.
- 5. W. M. Latimer, Oxidation Potentials, Prentice-Hall, Inc., Englewood Cliffs, NJ, 1952.
- 6. J. M. West, Basic Corrosion and Oxidation, Ellis Horwood Ltd., New York, 1980.
- 7. I. Ames, F. M. d'Heurle, and R. E. Horstmann, IBM J. Res. Develop. 14, 461 (1970).
- 8. S. Poon, J. T. Pan, T.-C. Wang, and B. Nelson, Proc. Tech. Program NEPCON'89 1, 426 (March 1989).
- 9. C.-K. Hu, M. B. Small, F. Kaufman, and D. J. Pearson,
- Mater. Res. Soc. Symp. Proc. 89, 369 (1990). 10. V. Brusic, M. Russak, R. Schad, G. Frankel, A. Selius, D. Dimilia, and D. Edmonson, J. Electrochem. Soc. 136, 42 (1989).
- 11. V. Brusic, J. Horkans, and D. J. Barclay, "Corrosion of Thin Film Storage Media: A Review," Electrochemistry in Transition from 20th to 21st Century, O. Murphy and S. Srinivasan, Eds., Plenum Press, New York, 1992.
- 12. V. Novotny and N. Staud, J. Electrochem. Soc. 135, 2931
- 13. P. B. P. Phipps and D. W. Rice, in Corrosion Chemistry, G. R. Brubaker and P. B. P. Phipps, Eds., American Chemical Society, Washington, DC, 1979, p. 235.
- 14. T. G. Wang and G. W. Warren, IEEE Trans. Magnetics MAG-24, 340 (1986).
- 15. K. Tagami and H. Hayashida, IEEE Trans. Magnetics MAG-23, 3648 (1987).
- 16. M. Rotel, J. Zahavi, H. C. N. Huang, P. A. Totta, and G. C. Schwartz, "Polarization of Al-Cu Conductive Lines on Oxidized Silicon Wafers," Proceedings of the First International Symposium on Corrosion of Electronic Materials and Devices, J. D. Sinclair, Ed., The Electrochemical Society, Inc., Pennington, NJ, 1991,
- 17. K. Hauffe, Oxidation of Metals, Plenum Press, New York, 1965.
- 18. R. Walker, J. Chem. Ed. 57, 789 (1980)
- 19. J. W. Mellor, Inorganic and Theoretical Chemistry, Longmans, Green & Co., New York, 1952, p. 148.
- 20. M. G. Fontana and N. D. Greene, Corrosion Engineering, McGraw-Hill Book Co., Inc., New York, 1967.
- 21. J. Grimblot and J. M. Eldridge, J. Electrochem. Soc. 129, 2366, 2369 (1982).
- 22. S. L. F. A. da Costa and S. M. L. Agostino, Corrosion 45, 472 (1989).
- 23. Procter and Gamble, Ltd., British Patent 652,339, December 1947
- 24. S. L. Cohen, V. Brusic, F. B. Kaufman, G. S. Frankel, Sh. Motakef, and B. M. Rush, J. Vac. Sci. Technol. A 8, 2417 (1990).
- 25. V. Brusic, M. A. Frisch, B. N. Eldridge, F. P. Novak, F. B. Kaufman, B. M. Rush, and G. S. Frankel, J. Electrochem. Soc. 138, 2253 (1991).
- 26. Cobratec Corrosion Control, PMC Specialties Group, division of PMC, Inc., Cincinnati, OH, 1990.

- 27. A. H. Roebuck, in Corrosion Inhibitors, C. C. Nathan, Ed., National Association of Corrosion Engineers, Houston, TX, 1973, p. 240.
- 28. G. C. Schwartz, Proceedings of the Fifth Symposium on Plasma Processing, G. S. Mathad, G. C. Schwartz, and C. Smolinsky, Eds., The Electrochemical Society, Pennington, NJ, Order No. PV85-1, 1965, p. 26.
- 29. C.-K. Hu, M. B. Small, and M. Schadt, Mater. Res. Soc. Symp. Proc. 76, 191 (1987).
- 30. J. L. Spencer, Solid State Technol. 27, 203 (1984).
- 31. G. Cameron and A. A. Chambers, Semiconductor International, p. 142 (May 1989).
- 32. C. R. M. Grovenor, in Microelectronic Materials, Adam Higler, Ed., ICP Publishing Co., Bristol, UK, 1989, p. 264.
- 33. V. Brusic, G. S. Frankel, C.-K. Hu, M. M. Plechaty, and B. M. Rush, Corrosion 47, 35 (1991)
- 34. W.-Y. Lee, J. M. Eldridge, and G. C. Schwartz, J. Appl. Phys. 52, 2994 (1981).
- 35. J. M. Eldridge, W.-Y. Lee, and G. C. Schwartz, U.S. Patent 4,368,220, 1983.
- 36. G. C. Schwartz and P. M. Schaible, J. Electrochem. Soc. 130, 1777 (1983).
- 37. K. Ohno, M. Sato, and Y. Arita, Jpn. J. Appl. Phys. 28, L1070 (1989).
- 38. B. J. Howard and Ch. Steinbruchel, Appl. Phys. Lett. 59, 914 (1991).
- 39. R. R. Thomas, V. Brusic, and B. M. Rush, "Correlation of Surface Wettability and Corrosion Rate for Benzotriazole-Treated Copper," J. Electrochem. Soc. 139, 678 (1992).

Received February 11, 1992; accepted for publication July 20, 1992

Vlasta Brusic IBM Research Division, Thomas J. Watson Research Center, P.O. Box 218, Yorktown Heights, New York 10598 (BRUSIC at YKTVMV, brusic@watson.ibm.com). Dr. Brusic is a Senior Engineer in the Manufacturing Research Department at the IBM Thomas J. Watson Research Center. She received a B.S. in chemical technology from the University of Zagreb, Croatia, in 1962, and a Ph.D. in physical chemistry from the University of Pennsylvania, Philadelphia, in 1971. She joined IBM in 1970, and has worked on materials and process aspects of gas display panels, gas lasers, and solder joints, and on the characterization of material surfaces with regard to corrosion. In 1992 she received an IBM Research Division Award for her work on the corrosion and protection of magnetic thin-film disks. Dr. Brusic is a member of The Electrochemical Society, the American Society for the Advancement of Science, and Sigma Xi.

Gerald S. Frankel IBM Research Division, Thomas J. Watson Research Center, P.O. Box 218, Yorktown Heights, New York 10598 (GSFRANK at WATSON, gsfrank@watson.ibm.com). Dr. Frankel is a Research Staff Member in the Manufacturing Research Department at the IBM Thomas J. Watson Research Center. He received an Sc.B. degree in materials science from Brown University in 1978. After working at Arthur D. Little, Inc. for two years, he attended the Massachusetts Institute of Technology and received an Sc.D. degree in materials science and engineering in 1985. He subsequently carried out postdoctoral research for one year at the Swiss Federal Technical Institute in Zurich. In 1986, Dr. Frankel joined IBM at the Thomas J. Watson Research Center, where he has primarily been studying the corrosion of thin films used in magnetic storage and electronic applications. He is a member of The Electrochemical Society.

Chao-Kyn Hu IBM Research Division, Thomas J. Watson Research Center, P.O. Box 218, Yorktown Heights, New York 10598 (CKHU at YKTVMZ, ckhu@watson.ibm.com). Dr. Hu is a Research Staff Member in the Silicon Technology Department at the IBM Thomas J. Watson Research Center. He received a B.S. degree from Chung Yuan College and an M.S. degree from the Institute of Physics, National Tsing Hua University, in Taiwan. He received a Ph.D. degree in physics from Brandeis University in 1979. Dr. Hu was a Research Associate at Rensselaer Polytechnic Institute before he joined IBM in 1984. His current research is in the areas of VLSI multilevel interconnection and Josephson integrated circuit fabrication. He is a coauthor of a book chapter and was a coinstructor for the short course entitled "Conductor Systems for VLSI" at the 1989 International VLSI Multilevel Interconnection Conference. Dr. Hu has published extensively in the areas of diffusion, electromigration, and chip fabrication. He has received two IBM Research Division Awards for his contributions to VLSI interconnection.

Miro M. Plechaty IBM Research Division, Thomas J. Watson Research Center, P.O. Box 218, Yorktown Heights, New York 10598 (PLECHAT at YKTVMZ). Dr. Plechaty is an Advisory Engineer in the Materials Characterization group of the Physical Sciences Department at the IBM Thomas J. Watson Research Center. He received a Diplom Chemist degree from the Technical University in Prague in 1960. He joined IBM in 1973, subsequently receiving a Ph.D. degree from the Union Institute in Cincinnati. His work has been on trace analytical ion chromatography and spectroscopy.

Geraldine Cogin Schwartz IBM Technology Products, East Fishkill facility, Route 52, Hopewell Junction, New York 12533. Dr. Schwartz retired from IBM in July 1992. She received her B.A. from Brooklyn College and her M.A. and Ph.D. from Columbia University. Dr. Schwartz was a Senior Engineer at the East Fishkill facility, where she had been engaged in research and development in many areas relating to thin-film technology. She consulted at the IBM facility in Poughkeepsie from 1964 to 1971, at which time she joined IBM. Dr. Schwartz is a Fellow of The Electrochemical Society and a member of Sigma Xi and the American Vacuum Society.

